Available online at www.sciencedirect.com

ScienceDirect

Procedia CIRP 58 (2017) 146 – 151

www.elsevier.com/locate/procedia

16th CIRP Conference on Modelling of Machining Operations

Mechanism of serrated chip formation in cutting process using digital image correlation technique

Wen-Jie Xu[a], Xiao-Ming Zhang[a]*, Jürgen Leopold[b], Han Ding[a]

[a]*School of Mechanical Science and Engineering, Huazhong University of Science and Technology, Wuhan 430074, China*
[b]*TBZ-PARIV GmbH, Chemnitz 09070, Germany*

* Corresponding author. Tel.: +86-2787559842; +86-2787559416. *E-mail address:* zhangxm.duyi@gmail.com

Abstract

Serrated chip, one of the major chip types in cutting process influences the quality of machined surface. However, the dynamic evolution of the serrated chip can hardly been quantitatively investigated, especially the fields of strain and stress in chip formation zone can hardly be detected. In this paper, the formation of serrated chip in machining Nickel aluminum bronze was captured by high-speed camera. The evolution history of displacement field during cutting process was obtained by the digital image correlation technique. Then the obtained displacement fields were treated as prescribed boundary conditions in finite element computation for strain and stress fields. Adopting the software Abaqus as a finite element computation platform, the strain and stress fields was observed, which can explain the formation of serrated chips from an experimental viewpoint. The work provided a new way to understand the mechanism of serrated chip formation in cutting process.

© 2017 The Authors. Published by Elsevier B.V. This is an open access article under the CC BY-NC-ND license (http://creativecommons.org/licenses/by-nc-nd/4.0/).
Peer-review under responsibility of the scientific committee of The 16th CIRP Conference on Modelling of Machining Operations

Keywords: Serrated chip; Digital image correlation; Strain field; Stress field; Metal cutting

1. Introduction

There are two main theories for the mechanism of serrated chip formation. One is the adiabatic shear theory, in which the serrated chip formation is attributed to a thermomechanical instability resulting in the concentration of large shear deformations in narrow layers [1]; another is the periodic brittle fracture theory, who thinks serrated chip formation is due to the occurrence of fracture in the outside of free surfaces [2].

Literature review reveals that the study of the serrated chip formation mostly focused on the analytical model and finite element method (FEM) simulation. Duan proposed a calculate model computing shear strain and shear strain rate within the shear band of serrated chips [3]. Yang developed an analytical solution of adiabatic shear band spacing and found the relationship between the adiabatic shear band spacing and cutting speed [4].

The formation of discontinuous chip in FEM simulations was first solved by applying ductile fracture criterion to Ti-6Al-4V alloy [5] and a two-phase brass [6] by Usui et al. Guo simulated the discontinuous chip of AISI 4340 by using the Johnson-Cook plastic model and used Johnson-Cook damage model to simulate the material crack propagation [7]. Wu used FEM simulation to prove that adiabatic effect is the key factor to lead to the serrated chip in high speed cutting of TC21 alloy [8].

However, it's hardly to observe the chip formation process directly, especially from the beginning of deformation to the completion of a chip. A traditional method was to place grids on the undeformed chips to observe deformation by comparing the grid shapes before and after cutting, which is, however, imprecise and loses the process information. Digital image correlation (DIC) is essentially a kind of non-rigid image matching technique, which is different from particle image velocimetry (PIV) for not only taking rigid body motion but also non-rigid body motion into consideration.

2212-8271 © 2017 The Authors. Published by Elsevier B.V. This is an open access article under the CC BY-NC-ND license (http://creativecommons.org/licenses/by-nc-nd/4.0/).
Peer-review under responsibility of the scientific committee of The 16th CIRP Conference on Modelling of Machining Operations
doi:10.1016/j.procir.2017.03.207

Hence, DIC is more suitable for measuring the plastic deformation of solid than PIV and the latter is mainly applied in measuring flow field. DIC has been used to measure the material deformation behavior in laboratory as a mature method, especially in the quasi-static simple tension test. With the promotion of Charge-coupled device (CCD) camera, it has also been used in cutting process observation recently. Guo et al. obtained strain rate and stain curves of materials passing the shear deformation zone by using DIC technique, they proposed a way to constrain chip formation process [9]. The varied chip morphologies under different rake angle were observed in situ study of flow dynamics by Guo et al [10]. Baizeau adopted double-frame camera to capture hard machining process at high cutting speed, the work focused on the surface under the machined surface [11], they also applied the DIC to segmented chip formation analysis and measured cutting forces at camera acquisition frequency [12].Dinakar and Koushik used DIC to observe the plastic flow in shear band by constraining the sliding phase [13]. Outeiro measured the residual plastic strain distribution of subsurface in orthogonal cutting experiment by DIC [14].

In this article, orthogonal cutting on nickel aluminum bronze (NAB) and Al7075T6 was implemented, where the serrated chip and continuous chip are generated, respectively. The cutting area was recorded by high-speed camera and the cutting force was measured by rotation dynamometer. By tracing the boundary of serrated chip, a direct description about the chip formation was presented. Then, DIC technique and finite element method (FEM) was combined together to obtain not only the displacement field but also the stress field and plastic strain field. With stress field, cutting force was computed by integrating the stress along the shear zone. In the end, for validating the experiment result, a comparison between cutting force measured and cutting force computed was proposed.

2. Experiment

2.1. Experimental set-up

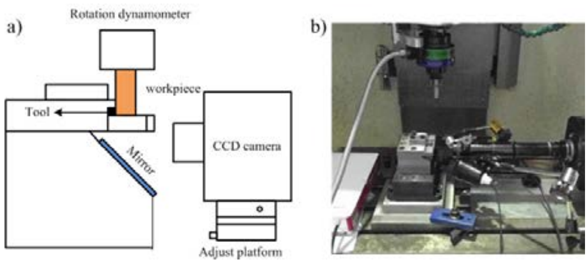

Fig. 1. a) Diagram b) Set-up

As shown in Fig. 1, Kistler 9123C rotation dynamometer and pco.dimax HD camera was adopted. The cylindrical workpiece was fixed with the rotation dynamometer for measuring cutting force. The mirror was positioned at an angel of 45 degrees to the horizontal plane to change the light path from vertical direction to horizontal direction. A laser beam was adopted to acquire adequate light intensity, so as to get images with high quality. A grooving tool with 4mm thickness was chosen. In order to obtain smooth surface, the tool was first ground by diamond grinding wheel, and then polished by diamond suspension for 15 minutes.

To get better result of DIC analysis, the surface quality was crucial. Although the surface of solid has natural texture, but in order to acquire adequate precision, NAB specimen was sandblasted by #1000 glass beads and AL7075T6 specimen was sandblasted by #2000 glass beads. This method can make sure the characteristic of image random enough and nearly isotropy in a small area.

The signal of rotation dynamometer and CCD camera were kept synchronized by external trigger equipment and the sample frequency was 10000Hz. The working parameters of camera are listed in Table 1.

Table 1. Camera parameters

Material	Frame rate	Scale/pixel	Image size
NAB	10000	1.506μm	624 x 500
AL7075T6	4000	1.506μm	960 x 720

2.2. Material and experiment parameters

NAB alloy (ZCuAl9Fe4Ni4Mn2) and Al7075T6 were chosen as specimen material. The Johnson-Cook constitutive model was chosen for its widely using in describing material plastic behaviour, the material parameters of NAB obtained from literature [15]:

$$\sigma = (A + B\varepsilon^n)\left[1 + C\ln\left(\frac{\dot{\varepsilon}}{\dot{\varepsilon}_0}\right)\right]\left[1 - \left(\frac{T - T_r}{T_m - T_r}\right)^m\right] \quad (1)$$

Table 2. Johnson−Cook constitutive parameters for NAB

A/MPa	B/MPa	n	C	m
295	759.5	0.405	0.011	1.09

Table 3. Johnson-Cook constitutive parameters for Al7075T6

A/MPa	B/MPa	n	C	m
295	759.5	0.405	0.011	1.09

Table 4. Cutting parameters

Material	NAB	Al7075T6
Cutting speed	1m/min	5m/min
Cutting thickness	0.08mm	0.05mm
Rake angle	15°	15°
Back angle	5°	5°

Download English Version:

https://daneshyari.com/en/article/5470241

Download Persian Version:

https://daneshyari.com/article/5470241

Daneshyari.com